Interaction of a Peptide Model of a Hydrophobic Transmembrane α-Helical Segment of a Membrane Protein with Phosphatidylethanolamine Bilayers: Differential Scanning Calorimetric and Fourier Transform Infrared Spectroscopic Studies

Yuan-Peng Zhang,* Ruthven N. A. H. Lewis,* Robert S. Hodges,*‡ and Ronald N. McElhaney*
*Department of Biochemistry and ‡MRC Group in Protein Structure and Function, University of Alberta, Edmonton, Alberta T6G 2H7 Canada

ABSTRACT High-sensitivity differential scanning calorimetry (DSC) and Fourier transform infrared (FTIR) spectroscopy were used to study the interaction of a synthetic α-helical hydrophobic transmembrane peptide, Acetyl-Lys_2-Gly-Leu_{24}-Lys_2-Ala-Amide, and members of a homologous series of *n*-saturated diacylphosphatidylethanolamines (PEs). In the lower range of peptide mol fractions, the DSC endotherms exhibited by the lipid/peptide mixtures consist of two components. The temperature and cooperativity of the sharper, higher-temperature component are very similar to those of pure PE bilayers and are almost unaffected by variations in the peptide/lipid ratio. However, the fractional contribution of this component to the total enthalpy change decreases with increases in peptide concentration, and this component completely disappears at higher peptide mol fractions. The other component, which is less cooperative and occurs at a lower temperature, predominates at higher peptide concentrations. These two components of the DSC endotherm can be attributed to the chain-melting phase transitions of peptide-nonassociated and peptide-associated PE molecules, respectively. Although the temperature at which the peptide-associated PE molecules melt is progressively decreased by increases in peptide concentration, the magnitude of this shift is independent of the length of the PE hydrocarbon chain. In addition, the width of the phase transition observed at higher peptide concentrations is also relatively insensitive to PE hydrocarbon chain length, except that peptide gel-phase immiscibility occurs in very short- or very long-chain PE bilayers. Moreover, the enthalpy of the chain-melting transition of the peptide-associated PE does not decrease to 0 even at high peptide concentrations, suggesting that this peptide does not abolish the cooperative gel/liquid-crystalline phase transition of the lipids with which it is in contact. The FTIR spectroscopic data indicate that the peptide remains in a predominantly α-helical conformation, but that the peptide α-helix is subject to small distortions coincident with the changes in hydrophobic thickness that accompany the chain-melting phase transition of the PE bilayer. These data also indicate that the peptide significantly disorders the hydrocarbon chains of adjacent PE molecules in both the gel and liquid-crystalline states relatively independently of lipid hydrocarbon chain length. The relative independence of many aspects of PE-peptide interactions on the hydrophobic thickness of the host bilayer observed in the present study is in marked contrast to the results of our previous study of peptide-phosphatidylcholine (PC) model membranes (Zhang et al. (1992) *Biochemistry* 31:11579–11588), where strong hydrocarbon chain length-dependent effects were observed. The differing effects of peptide incorporation on PE and PC bilayers is ascribed to the much stronger lipid polar headgroup interactions in the former system. We postulate that the primary effect of transmembrane peptide incorporation into PE bilayers is the disruption of the relatively strong electrostatic and hydrogen-bonding interactions at the bilayer surface, and that this effect is sufficiently large to mask the effect of hydrophobic mismatch between the lengths of the hydrophobic core of the peptide and its host bilayer.

INTRODUCTION

The mutual interactions of lipids and proteins are of fundamental importance for both the structure and function of biological membranes (see Gennis, 1989; Yeagle, 1992). For this reason there have been many studies of the interactions of membrane proteins with their host lipid bilayers, in both biological and reconstituted membrane systems, employing a wide variety of different physical techniques (see Watts and DePont, 1985, 1986; Cserháti and Szögyi, 1991, 1992, 1993; Epand and Epand, 1992; Selinsky, 1992). Although much valuable information has been derived from such studies, our understanding of the nature of lipid-protein interactions remains incomplete. This is due in part to the fact that most membrane proteins are relatively large, multidomain macromolecules of complex and usually unknown three-dimensional structure that can interact with lipid bilayers in complex, multifaceted ways (e.g., see McElhaney, 1986; Cserháti and Szögyi, 1991, 1992, 1993). To circumvent this

Received for publication 7 January 1994 and in final form 7 December 1994.

Address reprint requests to Dr. Ronald N. McElhaney, Department of Biochemistry, University of Alberta, Medical Sciences Building, Room 3-39, Edmonton, Alberta T6G 2H7 Canada. Tel.: 403-492-2413; Fax: 403-492-0095; E-mail: lewisr@gpu.srv.ualberta.ca.

0006-3495/95/03/847/11 $2.00

Abbreviations used in this article: P_{24}, Acetyl-Lys_2-Gly-Leu_{24}-Lys_2-Ala-Amide; PC, phosphatidylcholine; DPPC, dipalmitoylphosphatidylcholine; DSC, differential scanning calorimetry; FTIR, Fourier transform infrared; PE, phosphatidylethanolamine; C=O, carbonyl; T_m, gel/liquid-crystalline phase transition temperature; L_α, lamellar liquid-crystalline phase; L_β, lamellar gel phase; L_c, lamellar crystalline phase; NMR, nuclear magnetic resonance; ΔH, transition enthalpy (kcal/mol); R_p, peptide/lipid molar ratio; $\Delta T_{1/2}$, transition width measured at peak half-height. The hydrocarbon chains of the lipids used in this study are described by the shorthand notation *N*:0 with *N* representing the number of carbon atoms in the chain and 0 indicating the absence of carbon=carbon double bonds.

problem, a number of workers have synthesized peptide models of specific regions of natural proteins and have studied their interactions with the hydrophilic and/or hydrophobic regions of lipid bilayers (see Epand and Epand, 1992). Physical studies of such relatively tractable model membrane systems have already greatly advanced our understanding of the molecular basis of lipid-protein interactions.

The synthetic peptide Acetyl-Lys_2-Gly-Leu_{24}-Lys_2-Ala-Amide (P_{24}) and its analogues have been successfully used as models of the hydrophobic transmembrane α-helix of integral membrane proteins (Davis et al., 1983; Huschilt et al., 1985, 1989; Morrow et al., 1985; Pauls et al., 1985; Roux et al., 1989; Zhang et al., 1992a, b). These peptides contain a long sequence of hydrophobic leucine residues capped at both the N- and C-termini with two positively charged, relatively polar lysine residues. The polyleucine region of these peptides was designed to form a maximally stable α-helix, particularly in the hydrophobic environment of the lipid bilayer core. The lysine caps were designed both to anchor the ends of these peptides to the charged lipid polar headgroups at the surface of the lipid bilayer and to inhibit the lateral aggregation of these peptides. Indeed, a variety of physical techniques have provided evidence that these peptides do form stable α-helices that insert into PC model membranes perpendicular to the bilayer plane with the N- and C-termini exposed to the aqueous environment near the bilayer surface. Moreover, the incorporation of these peptides alters the thermotropic phase behavior of DPPC vesicles in the manner expected of a transmembrane α-helical protein and the rotational dynamics of the peptide itself are in turn sensitive to the fluidity and phase state of the host DPPC bilayer.

We have recently employed high-sensitivity DSC and FTIR spectroscopy to study the interaction of P_{24} and members of the homologous series of *n*-saturated diacyl PCs (Zhang et al., 1992b). At lower peptide concentrations, the DSC thermograms exhibited by the lipid/peptide mixtures are resolvable into two components. One of these components is fairly narrow, highly cooperative, and exhibits properties that are similar to but not identical with those of the pure lipid. In addition, the transition temperature of this component and its fractional contribution to the total enthalpy change decrease with an increase in peptide concentration, more or less independently of acyl chain length. The other component of the DSC endotherm is very broad and predominates at higher peptide concentrations. These two components were assigned to the chain-melting phase transitions of populations of peptide-nonassociated and peptide-associated lipid, respectively. Moreover, when the mean hydrophobic thickness of the PC bilayer is less than the peptide hydrophobic length, the peptide-associated lipid melts at higher temperatures than does the bulk lipid and vice versa. In addition, the chain-melting enthalpy of the broad endotherm does not decrease to 0 even at high peptide concentrations, suggesting that this peptide reduces but does not abolish the cooperative gel/liquid-crystalline phase transition of the lipids with which it is in contact. Our DSC results indicate that the width of the phase transition observed at high peptide concentrations is inversely but discontinuously related to hydrocarbon chain length and that gel phase immiscibility occurs when the hydrophobic thickness of the bilayer greatly exceeds the hydrophobic length of the peptide. The FTIR spectroscopic data indicate that the peptide forms a very stable α-helix under all of our experimental conditions but that small distortions of its α-helical conformation are induced in response to any mismatch between peptide hydrophobic length and bilayer hydrophobic thickness. These results also indicate that the peptide alters the conformational disposition of the acyl chains in contact with it and that the resultant conformational changes in the lipid hydrocarbon chains tend to minimize the extent of mismatch of peptide hydrophobic length and bilayer hydrophobic thickness.

Because all of the previous studies of P_{24}/lipid interactions were performed with PC bilayers, we wished to study the effect of variations of the phospholipid polar headgroup on the nature of these interactions. For this reason we repeated the above experiments using a homologous series of *n*-saturated diacyl PEs, and the results of this study are reported here. Perhaps surprisingly, the effect of P_{24} incorporation on the thermotropic phase behavior and hydrocarbon chain conformation of PE bilayers is in many ways quite different from its effects on PC bilayers. These results indicate that lipid polar headgroup structure may play an important role in determining the nature of the interactions between lipid bilayers and even a simple, prototypical α-helical transmembrane peptide.

MATERIALS AND METHODS

The *n*-saturated diacyl PEs were synthesized in this laboratory as described by Lewis and McElhaney (1993). The hydrophobic peptide P_{24} was synthesized using solid-phase methods and purified by high performance liquid chromatography as described by Davis et al. (1983). The pure peptide was then twice lyophilized from 10 mM hydrochloric acid to remove the trifluoroacetate counterions to which the peptide was bound at the end of the synthesis. This procedure was essential for samples used in FTIR spectroscopic experiments because trifluoroacetate exhibits a strong C=O absorption band near 1670 cm^{-1}, and this band overlaps both the ester C=O stretching band of the lipid and the amide I band of the peptide. Removal of the trifluoroacetate was not necessary with samples used in DSC experiments because the thermotropic properties of the peptide/PE mixtures were insensitive to its presence.

The PE/peptide vesicle suspensions used for DSC were prepared as follows. The lipid and the peptide were codissolved in chloroform/methanol (2:1) to obtain the required peptide/lipid ratio and, after removal of the solvent in a stream of nitrogen, the lipid/peptide mixture was lyophilized from benzene. The PE/peptide mixture was subsequently hydrated by vigorous vortexing with water at temperatures well above the T_m of the respective lipid to obtain a lipid concentration of 1–2 mg cm^{-3}. The DSC thermograms were recorded with a computer-controlled Microcal-MC2 high-sensitivity differential scanning calorimeter (Microcal Inc., Northampton, MA) operating at heating scan rates between 11 and 30°C h^{-1}. At these relatively slow scan rates the samples appear to be in thermal equilibrium and the heat capacity curves are scan rate independent. The data acquired were analyzed with DA2 and Origin software (Microcal Inc. and Microcal Software, Inc., respectively, Northampton, MA) and other computer programs available in the laboratory. Numerical data are generally reported ±1 SE. Standard errors were determined by averaging data obtained from different samples and from repeated scanning of individual samples. In cases

where the observed DSC thermograms clearly consisted of two or more overlapping peaks, curve-fitting methods were used to obtain estimates of the transition temperatures and enthalpies of the component peaks. The procedure used for the deconvolution of the DSC thermograms was based on the assumption that the observed thermogram can be described in terms of a linear combination of multiple independent transitions, each of which approximates a two-state transition.

Lipid/peptide samples for FTIR spectroscopy were either prepared freshly or from the samples used for DSC experiments. The first involved the preparation of a dry lipid/peptide sample as described above for the DSC sample except that chloroform-deuterated methanol (CH_3OD) (1:1, v/v) was used as the solvent. Alternatively, the sample used for DSC experiments was lyophilized and twice dissolved in deuterated methanol before being dried in vacuo overnight. The dry sample (containing 3–4 mg of lipid) was then hydrated with 50 μl of D_2O at temperatures well above the T_m of the respective lipid and then squeezed between the BaF_2 windows of a heatable liquid cell to form a 25-μm film and mounted in a cell holder attached to a computer-controlled circulating water bath that was used to regulate the temperature. Infrared spectra were recorded with a Digilab FTS-40 Fourier transform infrared spectrometer (Digilab Inc., Cambridge, MA) using the standard methodology for these types of samples (Mantsch et al., 1985). The data acquired were processed using DDS software (Digilab, Inc.) and other computer programs developed by the National Research Council of Canada. In cases where the spectra obtained consisted of broad overlapping bands, data processing usually involved the use of Fourier deconvolution to obtain fairly accurate estimates of the frequencies of the component bands, followed by application of curve-fitting procedures to the original spectra to obtain estimates of band width and integrated intensity. Typically band-narrowing factors of 1.4–2.0 were used during deconvolution. Under our conditions, band-narrowing factors of up to 2.5 could be used without introducing significant distortions to the spectra.

RESULTS

In considering the DSC and FTIR spectroscopic data presented below, it is important to compare the hydrophobic length of the P_{24} peptide with the hydrophobic thicknesses of the various PE bilayers used in this study. On the basis of measurements of a molecular model of this peptide in which its entire polyleucine core adopts an ideal α-helical conformation, we estimate that the mean hydrophobic length of P_{24} (the average length of the polyleucine sequence) is 31–32 Å. Given this value and the calculated hydrophobic thicknesses of the various PE bilayers in their gel and liquid-crystalline states (see Table 1), the following points should be noted. In the gel phase, the hydrophobic length of P_{24} exceeds the hydrophobic thickness of 11:0 and 12:0 PE but is progressively less than the hydrophobic thicknesses of the longer-chain PEs. In the liquid-crystalline phase, P_{24} hydrophobic length progressively exceeds the hydrophobic thickness of all PEs with hydrocarbon chains of 18 or fewer carbon atoms, but is slightly less than the hydrophobic thickness of the 20:0 PE bilayer. Thus, for the shorter-chain 11:0 and 12:0 PE, P_{24} hydrophobic length exceeds phospholipid bilayer thickness in both the gel and liquid-crystalline phases, while P_{24} hydrophobic length is always less than bilayer thickness for 20:0 PE. For the intermediate chain-length PEs (14:0–18:0 PE), the hydrophobic length of P_{24} is less than that of gel-state but more than that of the liquid-crystalline bilayer, with the best match of peptide and PE mean hydrophobic lengths occurring for 16:0 PE.

TABLE 1 Hydrophobic thicknesses of the bilayers formed by various PEs

PE	Hydrophobic thickness (Å)*		
	Gel phase	Liquid-crystalline phase	Mean‡
11:0	26.9	18.1	22.5
12:0	29.3	19.7	24.5
14:0	34.2	22.8	28.5
16:0	39.4	26.3	32.9
18:0	44.7	29.8	37.3
19:0	46.3	31.2	38.8
20:0	48.6	32.8	40.8

*Hydrophobic thicknesses were estimated using the equations used by Sperotto and Mouritsen (1988) to calculate the hydrophobic thicknesses of PC bilayers.

‡Mean of the hydrophobic thicknesses of the gel and liquid-crystalline phases.

Differential Scanning Calorimetry

Thermotropic phase behavior of the pure phosphatidylethanolamines

As illustrated in Fig. 1, unannealed aqueous dispersions of all the PEs studied here undergo a single fairly energetic and highly cooperative phase transition upon heating. This transition, which is completely reversible, arises from a conversion of the lamellar gel (L_β) to the lamellar liquid-crystalline (L_α) state. As expected, the T_m and ΔH of these chain-melting phase transitions increase progressively with increases in hydrocarbon chain length. For a thorough discussion of the thermotropic phase behavior of the complete homologous series of linear diacyl PEs, see Lewis and McElhaney (1993) and references cited therein.

Thermotropic phase behavior of peptide/phosphatidylethanolamine mixtures

Also illustrated in Fig. 1 are DSC heating scans of PE vesicles containing intermediate and high concentrations of

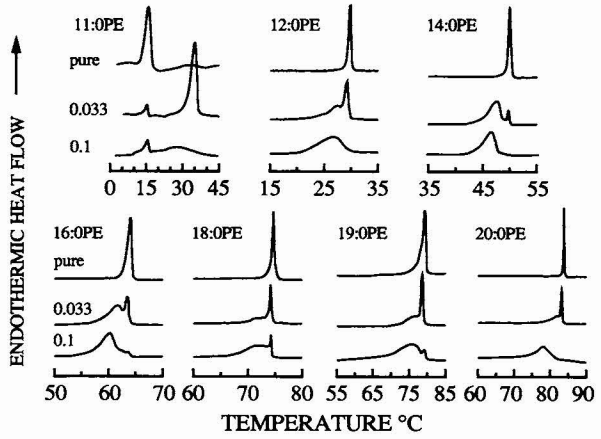

FIGURE 1 DSC heating thermograms of aqueous dispersion of the *n*-saturated diacyl PEs and their mixtures with P_{24}. The peptide/lipid ratios are indicated on the left.

P_{24}. Note that the overall thermotropic behavior of vesicles composed of P_{24} and 12:0 PE through 19:0 PE are similar. Specifically, as P_{24} concentration increases, a broad, lower-temperature DSC endotherm appears and grows in area at the expense of the sharp, higher-temperature endotherm, which eventually disappears entirely at higher R_p. The temperature of the broad DSC endotherm decreases with increasing P_{24} concentration, but that of the sharp component does not, corresponding instead to the T_m of the protein-free PE bilayers. Note also that the temperature difference between the broad and sharp DSC endotherms is the same for each PE bilayer at any given R_p value in all cases. Thus, despite the large variation in bilayer thickness relative to the hydrophobic length of P_{24}, the overall thermotropic phase behavior of all but the shortest and longest PEs examined is largely independent of the length of the phospholipid hydrocarbon chains and is dependent only on the peptide/lipid ratio. This finding is in contrast to the results of our previous study of the effects of P_{24} incorporation of the thermotropic phase behavior of a homologous series of linear disaturated PCs, where pronounced effects of phospholipid hydrocarbon chain length variations were observed (Zhang et al., 1992b). Thus, a detailed description of the qualitative and quantitative effects of P_{24} incorporation on the thermotropic phase behavior of 14:0 PE only will be provided, as this phospholipid is representative of most members of the homologous series of linear disaturated PEs. The somewhat different effects of P_{24} incorporation on the thermotropic phase behavior of the shortest and longest PEs studied will then be discussed separately.

Heating thermograms for P_{24}/14:0 PE mixtures are presented in Fig. 2 and the variation in T_m and ΔH as a function of R_p are presented in Fig. 3. The qualitative patterns shown therein typify those of mixtures of P_{24} with all of the intermediate chain length PEs used in this study. For any given lipid/peptide mixture the contours of the endotherms observed did not change with repeated scanning of the sample (typically three to four consecutive scans). As is evident from Fig. 2, pure 14:0 PE exhibits a single highly cooperative L_β/L_α phase transition centered at 49.9°C with a $\Delta T½$ of 0.5°C. With the incorporation of low to medium levels of P_{24} ($R_p = 0.0167 - 0.05$), the DSC thermograms appear to consist of two overlapping endothermic peaks. The higher-temperature peak is highly cooperative, is centered at temperatures slightly below the T_m of the pure lipid and, irrespective of R_p, its $\Delta T½$ and T_m remain fairly close to those of the pure lipid. However, the contribution of this higher-temperature component to the total enthalpy change decreases with increases in R_p and vanishes at R_p values in excess of 0.05 (see Fig. 3). In contrast, the properties of the lower-temperature component are markedly dependent upon R_p. This component is considerably broader than the higher-temperature component, its T_m decreases progressively with increases in R_p, and its contribution to the total ΔH increases with R_p increases such that it is the only resolvable component at high peptide/lipid ratios ($R_p > 0.05$) (see Fig. 3). Also, the magnitude of the decrease in the T_m of the broad component is insensitive to the length of the PE acyl chains and is dependent only upon the peptide/lipid ratio (see Fig. 4). These results are markedly different from those observed in comparable studies of PC/P_{24} mixtures, where the relative positions of these two peaks and the temperature difference between the peak maxima are correlated with the matching of peptide hydrophobic thickness and the mean hydrophobic thickness of the lipid bilayer (see Fig. 4 and Zhang et al.,

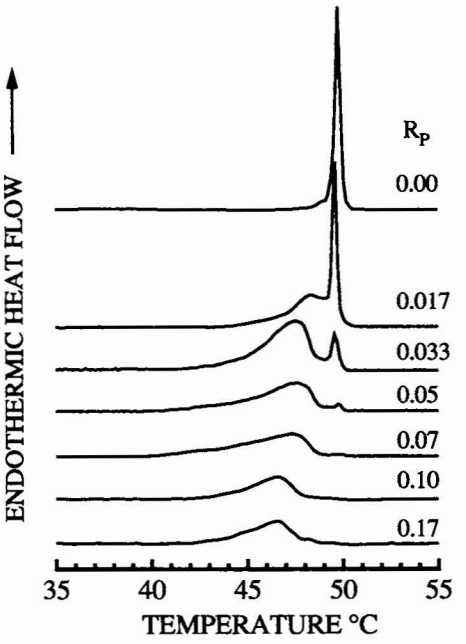

FIGURE 2 DSC heating thermograms of aqueous dispersions of 14:0 PE/P_{24} mixtures. The thermograms shown have been normalized with respect to lipid mass and scan rate. The R_p of each mixture is indicated to the right of each thermogram.

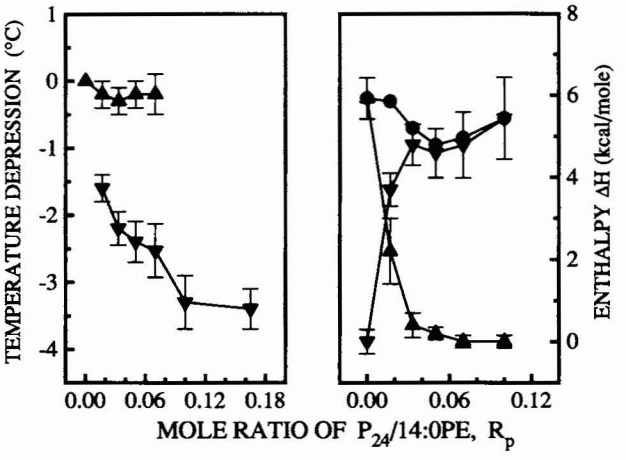

FIGURE 3 Effect of peptide/lipid ratio on the thermodynamic properties of the 14:0 PE/P_{24} mixtures. (*Left*) Variation of the peak temperatures of the sharp (▲) and broad (▼) components as a function of R_p. The temperatures are plotted as reduced temperatures relative to the peak melting temperature of the pure lipid. (*Right*) Variation of enthalpy of the sharp component (▲), broad component (▼), and the total enthalpy (●) as a function of R_p. Enthalpy values are quoted relative to the total amount of lipid in the sample.

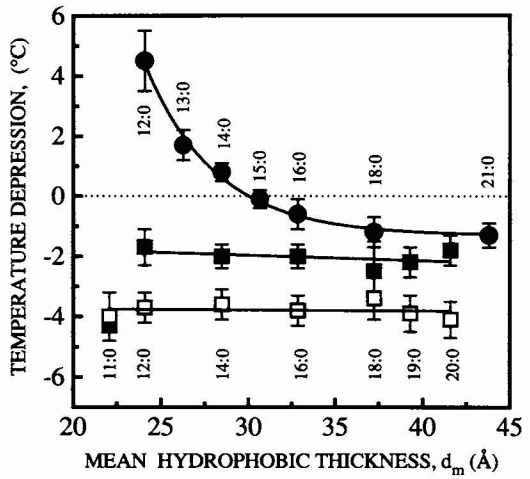

FIGURE 4 The relationship between mean bilayer hydrophobic thickness and the difference between the peak temperatures of the sharp and broad components of the DSC thermograms exhibited by PE- and PC-based lipid/P_{24} mixtures. For the PE-based peptide/lipid mixtures the R_p values are 0.033 (■) and 0.1 (□). The data on PC-based lipid/peptide mixtures (R_p = 0.033; ●) were obtained from Zhang et al. (1992b).

1992b). Moreover, the widths of the broad component observed in DSC thermograms of the PE/P_{24} mixtures are essentially independent of hydrocarbon chain length and exhibit a relatively weak dependence on R_p, properties also markedly different from those exhibited by PC/P_{24} mixtures (see Fig. 5). However, despite obvious differences between the PC- and PE-based lipid/P_{24} mixtures, it is clear that the general pattern of thermotropic phase behavior exhibited by both systems is more compatible with that of macroscopic mixtures of peptide-rich and peptide-poor domains than that of an ideal "two-dimensional solution" of the peptide in the lipid medium. If the existence of macroscopic mixtures of

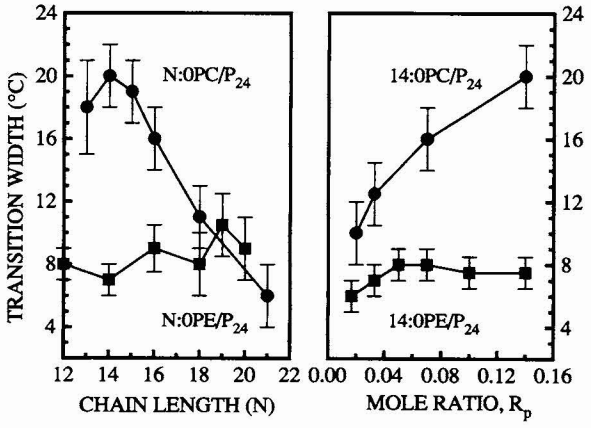

FIGURE 5 The chain-length dependence (*left*) and peptide concentration dependence (*right*) of the widths of the chain-melting transitions exhibited by broad components of PC- (●) and PE- (■) based P_{24}/lipid mixtures. The data shown were obtained from mixtures of R_p = 0.1 (*left*) and for 14:0 PC and 14:0 PE mixtures (*right*). The widths are measured from the starting temperature to the ending temperature of the endotherms of the broad components of the DSC endotherms.

peptide-rich and peptide-poor domains is assumed, then the obvious R_p dependence of the broad lower-temperature component of the DSC thermograms, and the fact that the properties of the sharp higher-temperature component are relatively insensitive to R_p, would suggest that the lower- and higher-temperature peaks of the DSC thermograms arise from the differential melting of peptide-rich and peptide-poor lipid domains, respectively. The rationale behind this assignment is the same as used in previous studies of PC/P_{24} mixtures (see Morrow et al., 1985; Zhang et al., 1992b).

Although the thermotropic phase behavior of mixtures of P_{24} with the *n*-saturated diacyl PEs seems to be generally independent of hydrocarbon chain length, the behavior of mixtures that contain PEs with very short and with very long fatty acyl chains differs somewhat from the general trends described above. For example, with 11:0 PE the peak assigned to the peptide-poor component exists as a major component of the DSC thermogram even at high R_p, in marked contrast to the other PEs for which peptide-poor domains make only a small contribution to the total enthalpy change measured at high R_p (see Fig. 1). The persistence of relatively large amounts of peptide-poor domains of 11:0 PE at high R_p is probably the result of lateral phase separation (see below). Also, at high R_p values, the contours of the DSC thermograms of mixtures of P_{24} with 20:0 PE change significantly with repeated scanning (see Fig. 7) in marked contrast to comparable mixtures with the short- and medium-chain PEs, which exhibit essentially identical DSC endotherms upon repeated scanning. For example, with 20:0 PE mixtures (R_p = 0.1) the first heating scan normally contains a minor peak component near 82°C and a broad component centered near 79°C. In subsequent scans the small peak near 82°C disappears and there is a downward shift in the T_m of the broad component. These changes in the contours of the DSC thermograms cannot be attributed to hydrolytic degradation of the lipids because thin-layer chromatographic analyses performed after the completion of the DSC experiment show no evidence of sample hydrolysis. A similar trend was also observed with 19:0 PE/P_{24} mixtures at high R_p, although the magnitude of these effects was considerably smaller. These observations indicate that mixtures of P_{24} with the longer-chain PEs are not as stable upon repeated heating and cooling as those with the medium-chain homologues. These findings also suggest that in mixtures of P_{24} with the 19:0 or 20:0 PE, there may initially have been lipid-protein lateral phase separation that disappears or is at least reduced upon repeated cycling through the phase transition temperature region. Evidence for peptide (Zhang et al., 1992b) or protein (Lewis and Engelman, 1983; Riegler and Möhwald, 1986) phase separation in long-chain PC bilayers has been reported previously. Interestingly, however, P_{24}/21:0 PC mixtures seem initially well mixed but exhibit an increasing degree of lateral phase separation upon repeated heating and cooling, just the opposite behavior to that exhibited by the long-chain PEs. The possible reasons for the lateral phase separation in bilayers of long-chain phospholipid will be explored in the Discussion section.

In addition to the chain length-dependent phase behavior manifested at the extremes of PE hydrocarbon chain lengths studied here, another chain length-dependent effect is manifested in a progressive fashion over a wider range of PE hydrocarbon chain lengths. Specifically, when plots of the total enthalpy as a function of R_p for all the PEs are compared (see Fig. 6), we find that with the short-chain PEs, the total ΔH decreases with R_p over the entire R_p range studied, whereas with most of the longer-chain PEs (N = 14–20) there is an initial decrease in total ΔH at low R_p followed by an apparent increase in the total ΔH in the high range of R_p values. This latter increase in ΔH is only observed at high R_p and seems to be due to the occurrence of a very broad thermotropic event underlying the hydrocarbon chain-melting phase transition of the PE/P_{24} mixtures (see Fig. 7). The manifestation of this additional broad thermotropic event becomes progressively more pronounced as the chain length of the host PE increases from 14 to 20 carbon atoms. These results contrast with those obtained for PC bilayers, where the incorporation of P_{24} progressively decreases ΔH to a comparable extent for all except the longest hydrocarbon chain length studied (Zhang et al., 1992b). The possible molecular basis of the appearance of these additional thermotropic events will be addressed in the Discussion section.

In the case of the short-chain PEs, incubation of aqueous dispersions of the pure lipids at low temperatures results in the formation of highly ordered L_c phases that melt directly to the liquid-crystalline phase at temperatures well above those of their typical L_β/L_α phase transitions (see Lewis and McElhaney, 1993, and references cited therein). In these studies, we also find that stable L_c phases can be formed from

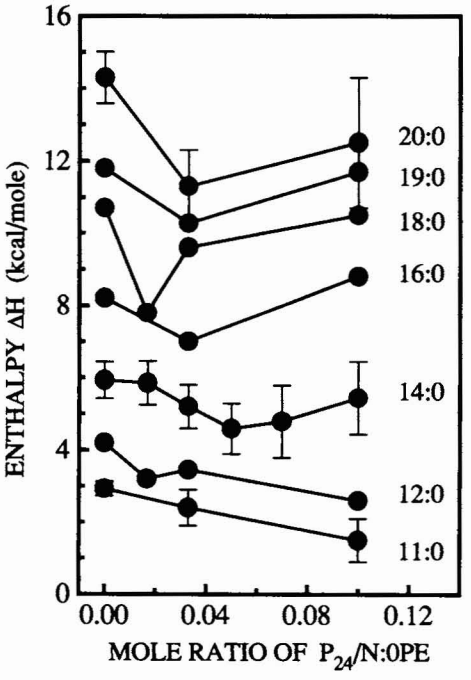

FIGURE 6 Variation of the overall transition enthalpies for mixtures of P_{24} with the *n*-saturated diacyl PEs as a function of R_p.

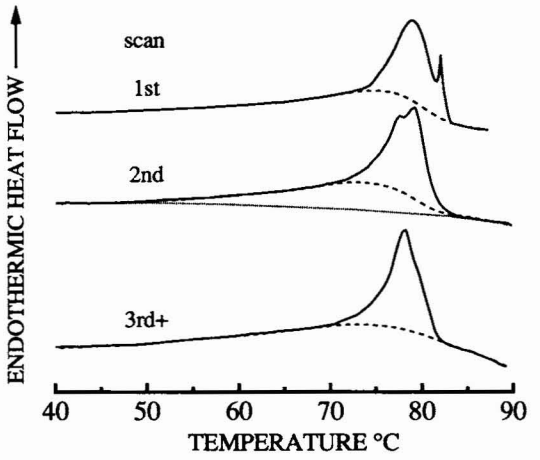

FIGURE 7 DSC thermograms of a 20:0 PE/P_{24} mixture (R_p = 0.1) recorded in consecutive scans over several days. The sample was stored at room temperature in between scans. In each thermogram the dashed line shows the baseline against which the enthalpy of the lipid chain-melting phase transition was estimated. The onset and completion temperatures of the lipid chain-melting phase transition were estimated with the aid of FTIR spectroscopy. The dotted line in the second thermogram is a representative instrument baseline, which is shown to emphasize the broad thermotropic event underlying the lipid chain-melting phase transition.

mixtures of P_{24} with the shorter-chain PEs (evidence presented below). With aqueous dispersions of pure 11:0 PE, prolonged incubation (several days) at low temperatures usually results in the suppression of the L_β/L_α chain-melting phase transition ($T_m \cong 16°C$) and its replacement by the more energetic L_c/L_α phase transition centered near 36°C (Lewis and McElhaney, 1993). For the 11:0 PE/P_{24} mixtures studied, our DSC data also indicate that endotherms corresponding to the L_β/L_α phase transition are suppressed after periods of low-temperature incubation and are replaced by more energetic endothermic transitions near 36°C (see Fig. 8). FTIR spectroscopic studies of these lipid/peptide mixtures indicate that the latter correspond to the melting of the L_c phase of this lipid (see below). Interestingly, our results also suggest that the presence of small amounts of P_{24} accelerates the rate at which the L_c phase forms in 11:0 PE bilayers. Thus, as shown in Fig. 8, samples of the pure 11:0 PE show no trace of L_c phase formation after 1 h incubation at 0–4°C. However, 11:0 PE/P_{24} mixtures of $R_p \cong 0.033$ form substantial amounts of the L_c phase upon similar treatment, although this effect becomes less pronounced at higher R_p values. Note that the tendency for low levels of P_{24} to accelerate the rate at which L_c phase forms is not observed with the longer-chain PEs, where the presence of P_{24} actually decreases both the rate and extent of formation of the L_c phase. Thus, with 14:0 PE, e.g., only trace amounts of the L_c phase were observed in the presence of P_{24} despite prolonged incubation (several days) at 0–4°C, and substantial conversion to the L_c phase only occurred with repeated application of the freeze-thaw procedures described by Lewis and McElhaney (1993). The fact that the L_c phases of the shorter-chain lipids can form in the presence of P_{24} is significant because it provides direct evidence for the phase separation of pure lipid domains from the

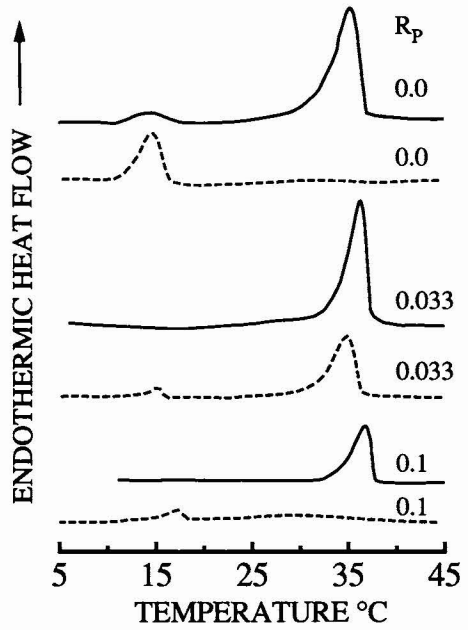

FIGURE 8 Effect of low-temperature incubation on the thermotropic phase behavior of 11:0 PE/P_{24} mixtures. The solid lines indicate the thermogram observed after overnight incubation at 0–4°C and the dashed lines indicate the thermograms obtained 1 h after cooling from liquid-crystalline temperatures to 0–4°C. The R_p values are indicated at the right of each thermogram.

peptide. Recent NMR and FTIR spectroscopic studies of the L_c phases of the *n*-saturated diacyl PEs have indicated that these are highly ordered structures in which there are strong lateral interactions between the hydrocarbon chains and strong intermolecular electrostatic and hydrogen-bonding interactions between moieties of the polar headgroup (Lewis and McElhaney, 1993). Because the formation of these L_c phases involves the formation of local extended arrays of pure PE, the fact that gel-phase mixtures of P_{24} with the short-chain PEs are very prone to form such structures suggests peptide/lipid phase separation. The implications of this conclusion will be further explored in the Discussion section.

FTIR spectroscopy

In these studies, infrared spectra of mixtures of the peptide with the homologous series of linear saturated diacyl PEs were recorded as a function of temperature and as a function of the mol ratio of the peptide. The use of FTIR spectroscopy permits a noninvasive monitoring of both the structural organization of the lipid bilayer and the conformation of the peptide. Thus, the gel/liquid-crystalline phase transitions of the lipid bilayer can be conveniently monitored by changes in the frequency of CH_2 symmetrical stretching band near 2850 cm^{-1}, changes in solid-state hydrocarbon chain packing by changes in the CH_2 scissoring band near 1468 cm^{-1}, changes in the hydration and/or polarity of the polar/apolar interfacial region of the lipid bilayer by changes in the contours of the ester carbonyl stretching bands near 1735 cm^{-1}, and changes in peptide structure by changes in the conformationally sensitive amide I band near 1650 cm^{-1} (see Mendelsohn and Mantsch, 1986; Mantsch and McElhaney, 1991).

Illustrated in Fig. 9 are the frequency changes exhibited by the lipid hydrocarbon chain CH_2 symmetrical stretching and the peptide amide I bands as a function of temperature for the 11:0 PE/P_{24}, 14:0 PE/P_{24}, 16:0 PE/P_{24}, 18:0 PE/P_{24}, and 20:0 PE/P_{24} mixtures with $R_p = 0.10$. Plots of the frequency of the CH_2 symmetrical stretching band of the pure PEs are also included for comparison. DSC endotherms of these PE/P_{24} mixtures are also included in Fig. 9 to facilitate comparison of the calorimetric and FTIR spectroscopic results. The DSC endotherm is accompanied by an increase in the frequency of the lipid hydrocarbon chain CH_2 symmetrical stretching band near 2850 cm^{-1}. This result confirms that even at high R_p the DSC endotherm is still monitoring a cooperative chain melting of the PE hydrocarbon chains, given that increases in frequency of 2–3 cm^{-1} invariably accompany the conversion of an all-*trans* hydrocarbon chain to one containing a number of *gauche* rotational isomers. In addition, these mixtures also exhibit relatively sharp amide I vibrational bands near 1655 cm^{-1}, consistent with a predominantly α-helical conformation of the peptide in the lipid bilayer (see Zhang et al., 1992a and references cited therein). However, we also find that a small decrease in the frequency of the amide I band of the peptide consistently occurs at the chain-melting phase transition of all PE/P_{24} mixtures studied. For mixtures containing the short- to medium-chain PEs ($N \leq 16$), the magnitude of this frequency shift is very small but increases significantly with the longer-chain lipids (see Fig. 9). The magnitude of this frequency shift also decreases with increasing R_p (data not shown). This frequency change is both reproducible and reversible, suggesting that the conformation of the peptide is slightly altered at the gel/liquid-crystalline phase transition of the host PE bilayer. However,

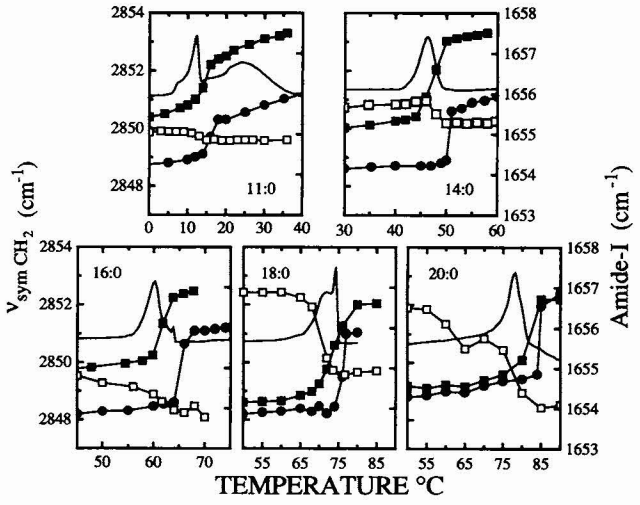

FIGURE 9 Temperature dependence of the symmetrical CH_2 stretching (●,■) and amide I (□) absorption bands exhibited by *N*:0 PE/P_{24} mixtures. Data are presented for pure lipid (●) and PE/P_{24} mixtures of $R_p = 0.1$ (■) of the PEs indicated. The DSC thermograms of the respective PE/P_{24} mixtures of $R_p = 0.1$ are included for comparison.

since this peptide retains a predominantly α-helical conformation in a variety of different environments and over a wide range of temperature (Zhang et al., 1992a), these small-frequency shifts probably represent minor distortions of the peptide α-helix (Chirgadze et al., 1976). Interestingly, when P_{24} is dispersed in the gel phase of the longer-chain PEs, the frequency of the amide I band tends to be higher than that expected of so-called "relaxed" α-helices (see Chirgadze et al., 1976). Thus, the small distortions of the peptide conformation in these systems may well be attributable to the dispersal of the peptide in thick gel-phase lipid bilayers. Qualitatively similar results have been reported previously for PC/P_{24} mixtures (Zhang et al., 1992b).

The effects of peptide incorporation on the hydrocarbon chain organization of the host PE bilayers in both the gel and liquid-crystalline states were also investigated by FTIR spectroscopy. With the exception of mixtures involving 20:0 PE, the frequencies of the symmetrical CH_2 stretching bands observed in the gel and in the liquid-crystalline states of the P_{24}/PE mixtures are always higher than that of the pure lipid (see Fig. 9), regardless of the length of the PE hydrocarbon chains. Because increases in the frequency of this band are associated with increases in hydrocarbon chain conformational disorder (see Mendelsohn and Mantsch, 1986; Mantsch and McElhaney, 1991), these results indicate that the interaction of P_{24} with PE bilayers results in an overall increase in the conformational disorder of the hydrocarbon chains both above and below the PE phase transition temperature. This effect seems more pronounced with the short- to medium-chain lipids ($N \leq 16$). Interestingly, at high R_p the CH_2 symmetrical stretching frequencies observed in the gel and liquid-crystalline states of these PE/P_{24} mixtures are comparable to those observed in pure PC bilayers (see Zhang et al., 1992b). This suggests that hydrocarbon chain conformational disorder in both the gel and liquid-crystalline states of the P_{24}/PE mixtures is comparable to that found in the corresponding phases of pure PC bilayers. The incorporation of P_{24} into PC bilayers generally produces only a slight but chain length-dependent increase in hydrocarbon chain conformational disorder in the gel and liquid-crystalline states (Zhang et al., 1992b).

The FTIR spectra shown in Fig. 10 were acquired at 0°C and were obtained from a 11:0 PE/P_{24} mixture of $R_p = 0.1$ before and after low-temperature incubation of the samples. Before low-temperature incubation of the sample, the C=O stretching band of the ester groups of the lipids has an asymmetrical band contour with a maximum near 1735 cm^{-1} and a broad lower-frequency shoulder that extends well below 1700 cm^{-1} and overlaps with the upper wings of the amide I band of the peptide (see Fig. 10, top left). Also, before low-temperature incubation of the sample, the main CH_2 scissoring band is a single absorption peak centered near 1468 cm^{-1} (Fig. 10, top right). These features are typical of the L_β gel phases formed by pure samples of the *n*-saturated diacyl PEs (see Lewis and McElhaney, 1993). Fig. 10 also shows that these features change significantly after low-temperature incubation of the sample for 2 days. In the ester

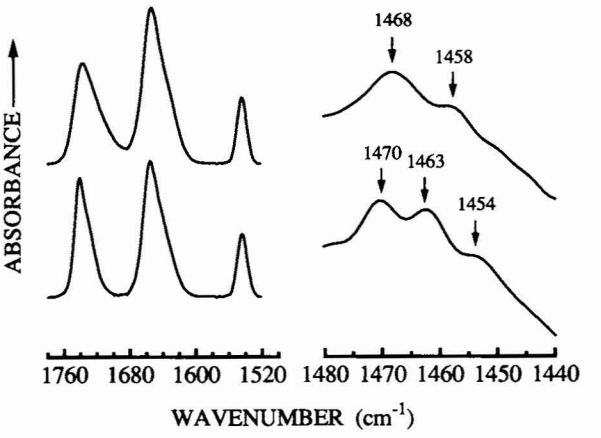

FIGURE 10 FTIR spectra of gel (*top*) and crystalline phases (*bottom*) formed by a mixture of P_{24} with 11:0 PE ($R_p = 0.1$). The spectra are shown in the absorbance mode with the left panel indicating the contours of the ester C=O stretching bands of the lipid as well as the amide I and amide II bands of the peptide, and the right panel indicating the contours of the CH_2 scissoring bands of the lipid hydrocarbon chains. The spectra of the CH_2 scissoring bands have been enhanced by a band narrowing factor of 1.4. The absorption band near 1456 cm^{-1} arises from the asymmetrical bending vibration of the end methyl groups of the hydrocarbon chain.

C=O stretching region of the spectrum, the lipid C=O stretching band narrows considerably and the resulting contours consist of a sharp absorption peak near 1742 cm^{-1} and a shoulder near 1735 cm^{-1} (Fig. 10, bottom left), whereas in the CH_2 deformation region of the spectrum, the main CH_2 scissoring band is split into two components centered near 1472 cm^{-1} and 1466 cm^{-1}. These features are similar to those observed in the stable L_c phases formed by pure samples of the *n*-saturated diacyl PEs (see Lewis and McElhaney, 1993). Thus it is evident that despite the presence of a substantial quantity of P_{24}, a significant fraction of the lipid component of the 11:0 PE/P_{24} mixture spontaneously assembles into structures similar to the stable L_c phases of the pure lipid when the sample is incubated at low temperatures. Given the strong lipid-lipid interactions characteristic of the stable L_c phases of the *n*-saturated diacyl PEs (see Lewis and McElhaney, 1993 and references cited therein), this result provides further evidence for phase separation of the short-chain PEs from the peptide.

DISCUSSION

In this study we find that at low to medium R_p, PE/P_{24} mixtures exhibit multicomponent DSC thermograms that can be resolved into two components. The narrow higher-temperature component exhibits properties that are essentially insensitive to R_p, but that are similar to those of the pure lipid, whereas the broader low-temperature component exhibits properties that vary with the lipid/peptide ratio. Moreover, the contribution of the sharper component to the total enthalpy change decreases and that of the broader component increases with increases in R_p and, for the most part, the sharp component tends to vanish when R_p exceeds values of 0.05.

The latter R_p value corresponds to a peptide/lipid ratio of 20:1, a value comparable to that estimated for the formation of a single unique lipid solvation layer around each peptide molecule (see Morrow et al., 1985). It is also evident from Fig. 1 that remnants of the sharp component can often be resolved in the DSC thermograms of P_{24}/PE mixtures ($N \geq 16$) at higher R_p values. We believe that the latter observation is a result of the phase separation that probably occurs when such mixtures are cooled to temperatures well below T_m (see below). In principle, the general pattern of two-component DSC thermograms exhibited by these PE/peptide mixtures can be rationalized by postulating the existence of macroscopic mixtures of peptide-rich and peptide-poor lipid domains. If such behavior is assumed, one can assign the lower-temperature and higher-temperature DSC peaks to the differential melting of peptide-rich and peptide-poor lipid domains, respectively, as described elsewhere for PC/P_{24} mixtures (see Zhang et al., 1992b). Alternatively, the two components of the DSC endotherm could be postulated to arise from a single process occurring in a macroscopically homogenous system, in which case temperature/composition pseudo-phase diagrams could be constructed from the calorimetrically determined onset and completion temperatures of the DSC endotherms, and interpreted accordingly. The sample preparation methodology used here normally produces macroscopically homogenous samples. Unfortunately, because of the high T_ms and tendencies of PEs to crystallize at temperatures below T_m, these lipid-peptide samples do not easily lend themselves to the usual verification protocols (e.g., density gradient centrifugation) and, as a consequence, it is difficult to confirm that these samples are macroscopically homogenous. Therefore, rigorous interpretation of this aspect of the behavior of these lipid/peptide mixtures is best deferred until the molecular basis of the appearance of these two-component DSC endotherms has been firmly established.

Although there are some similarities between this work and previous studies of PC-based P_{24}/lipid mixtures, the dominant feature of this study is the marked difference between the effects of P_{24} on the PC and PE lipid bilayers. Indeed, for most of the PE/peptide mixtures studied, the overall pattern of thermotropic phase behavior observed is essentially the same and is determined primarily by the lipid/peptide ratio rather than the match of peptide hydrophobic length and lipid bilayer thickness. This unexpected result is not predicted with current theoretical models of the interaction of lipid bilayers with hydrophobic transmembrane proteins/peptides (see Owicki and McConnell, 1979; Mouritsen and Bloom, 1984; Riegler and Möhwald, 1986; Peschke et al., 1987; Sperotto and Mouritsen, 1988, 1991). We believe, however, that our data can be satisfactorily rationalized on the basis of differences in the relative contributions of headgroup/headgroup interactions to the free energy of stabilization of the respective bilayers (see below).

An important difference between the thermotropic phase behavior of PC- and PE-based P_{24} mixtures is that the T_ms of the broad components of the latter always occur some 3–4°C below those of the sharp components regardless of the chain length (or hydrophobic thickness) of the host PE bilayer (see Fig. 4). In principle, the intrinsic differences between the properties of PE and PC bilayers could explain why the thermotropic phase behavior is apparently insensitive to the mismatch of peptide hydrophobic length and bilayer hydrophobic thickness in PE but not in PC bilayers. It is now generally accepted that relatively strong electrostatic and hydrogen-bonding headgroup-headgroup interactions contribute significantly to the stabilization of PE bilayers, whereas such interactions are much weaker in PC bilayers (see Nagle, 1976; Boggs, 1980, 1986, 1987; Lewis and McElhaney, 1993). Thus, at the surfaces of hydrated PE bilayers, the phosphoryl ethanolamine headgroups probably form part of a dynamic network of intermolecular electrostatic and hydrogen-bonding interactions involving the amino and phosphate moieties of the headgroups as well as the surrounding water molecules. We therefore suggest that the observed decrease in T_m coincident with the introduction of P_{24} into PE bilayers can be directly attributed to its disruption of the hydrogen-bonding network, because the access of any PE molecule to potential hydrogen-bonding partners is substantially reduced by its proximity to and contact with the peptide. Most probably this effect is a function of R_p, and given the importance of the integrity of the hydrogen-bonding network to the stability of PE bilayers, it may well be large enough to effectively mask most effects attributable to the mismatch of peptide hydrophobic length and bilayer hydrophobic thickness. It is also possible that the positively charged lysine residues on the ends of the peptide may locally disrupt the attractive electrostatic interactions between adjacent PE molecules in the bilayers.

Although effects attributable to a mismatch of peptide hydrophobic length and bilayer hydrophobic thickness were not dominant factors in these studies, hydrophobic mismatch may affect certain aspects of the phase behavior of P_{24} mixtures with the short- and long-chain PEs. For example, the incorporation of extraneous molecules (cholesterol, proteins, etc.) into phospholipid bilayers generally inhibits L_c phase formation, presumably by interfering with the close packing of lipid molecules required for the nucleation and growth of such highly ordered, partially dehydrated, quasi-crystalline structures (see McElhaney, 1982). Such an effect is actually observed upon incorporation of P_{24} into bilayers composed of the medium- and long-chain PEs. In contrast, however, the incorporation of low to moderate levels of P_{24} into the short-chain PE actually promotes the formation of the L_c phase when these systems are incubated at low temperatures. These observations can be rationalized by considerations of the probable effects of hydrophobic mismatch on the miscibility of P_{24} with gel-phase lipids. With lipids such as 11:0 PE, the hydrophobic thickness of the gel-phase bilayer is significantly less than the hydrophobic length of P_{24} (see Table 1), which could result in exposure of a portion of the hydrophobic polyleucine core of P_{24} to water. The destabilizing effect of the exposure of the hydrophobic region of P_{24} to water could be minimized by the lateral aggregation (i.e.,

phase separation) of P_{24} within the gel-state bilayer. For lipid/P_{24} mixtures composed of the shorter-chain PEs, this process of lipid/peptide phase separation may also be promoted because of weaker hydrophobic and van der Waals interactions between the polyleucine α-helix and the short hydrocarbon chains of the lipid molecule. Most probably, the processes described above result in the formation of domains of virtually pure lipid, a prerequisite for the formation of the lipid L_c phase, which forms when mixtures of P_{24} with the short-chain lipids are cooled to temperatures below T_m. Indeed, with such mixtures, the presence of exposed hydrophobic surfaces of the peptide may even enhance the crystallization of the lipid by providing dehydrated nucleation sites at which L_c phase formation can be initiated. With the medium-chain PEs (14:0–18:0 PE), however, the tendency toward lipid-peptide phase separation will probably be reduced because of a closer matching of mean bilayer hydrophobic thickness and peptide hydrophobic length (see Table 1). Thus, such mixtures should be more stable because the reduced exposure of the hydrophobic core of P_{24} to water, and because hydrophobic interactions between the PE hydrocarbon chains and the hydrophobic surfaces of the peptide α-helix increase with increasing hydrocarbon chain length. Most probably such factors inhibit the formation of the PE L_c phase by significantly attenuating tendencies toward PE/peptide phase separation.

Peptide-phospholipid hydrophobic mismatch in the gel phase may also provide an explanation for the unusual biphasic dependence of ΔH on R_p exhibited by the medium- and long-chain PEs in the present study. From previous studies of integral membrane protein/phospholipid systems, one expects that the incorporation of increasing amounts of protein into a lipid bilayer should result in a progressive decrease in the ΔH values of the lipid chain-melting phase transition (see McElhaney, 1986). Indeed, this is exactly what is observed when P_{24} is incorporated into PCs of varying hydrocarbon chain lengths (see Zhang et al., 1992b) and upon incorporation of P_{24} into the shorter-chain PEs (this work). However, incorporation of increasing quantities of P_{24} into medium- and long-chain PEs results in an apparent increase in ΔH after an initial decrease. Given that it is unlikely that increases in P_{24} concentration could result in an increase in the ΔH of hydrocarbon chain melting, another explanation for the biphasic dependence of ΔH on R_p for the medium and long PEs must be sought. We note that the anomalous dependence of ΔH on R_p is observed for all PEs for which the hydrophobic thickness of the gel-phase bilayer exceeds the hydrophobic length of the peptide. We also note that, particularly with the longer-chain PEs, the DSC endotherms actually appear to consist of a more cooperative component superimposed on a less cooperative component, the latter manifested as a curvature in the baseline of the calorimetric trace in the general region of the gel to liquid-crystalline phase transition. Since the FTIR results identify the sharper component as the lipid hydrocarbon chain-melting event, we propose that the broader component results from the heat absorbed by the "dissolution" of aggregated peptide present in the gel-state bilayer in the thinner and more disordered liquid-crystalline phospholipid domains formed near the T_m. Since this latter process would be expected to become quantitatively more important both with increases in R_p and with increases in the hydrocarbon chain length, this hypothesis seems compatible with the experimental observations. Moreover, the fact that this behavior is manifested in the PC homologous series only at very long hydrocarbon chain length is also compatible with this suggestion, because the more disordered gel phase of PC bilayers would be expected to attenuate the effects of hydrophobic mismatch on the gel-phase miscibility of P_{24}.

Finally, this study and that of Zhang et al. (1992b) demonstrate that the nature of the lipid polar headgroup is an important determinant of how the behavior of bilayer lipid molecules is affected by membrane-penetrating proteins/peptides even when lipid-peptide interactions are expected to be primarily hydrophobic. This is probably because the presence of the peptide/protein may disrupt the pattern of hydrogen-bonding and/or ionic interactions in the lipid bilayer, even in the absence of specific interactions between the protein/peptide and the polar headgroups of the lipid. Thus, the nature of the interaction of even simple hydrophobic peptides such as P_{24} with lipid bilayers depends on the relative strengths of hydrogen-bonding and ionic interactions at the bilayer surface, in addition to changes in hydrocarbon chain conformation and packing in the hydrophobic domain of the lipid bilayer. To date, such ideas have not been the focus of much theoretical or experimental study, and our data clearly indicate that these factors will have to be examined before the complexities of the interaction of lipids and transmembrane proteins can be fully understood.

This work was supported by operating and major equipment grants from the Medical Research Council of Canada, by major equipment grants from the Alberta Heritage Foundation for Medical Research, and by an operating grant from the University of Alberta Central Research Fund.

REFERENCES

Boggs, J. M. 1980. Intermolecular hydrogen bonding between lipids: influence on organization and function of lipids in membranes. *Can. J. Biochem.* 58:755–770.

Boggs, J. M. 1986. Effect of lipid structural modifications on their intermolecular hydrogen bonding interactions and membrane function. *Biochem. Cell Biol.* 64:50–57.

Boggs, J. M. 1987. Lipid intermolecular hydrogen bonding: influence on structural organization and membrane function. *Biochim. Biophys. Acta.* 906:353–404.

Cserhåti, T., and M. Szögyi. 1991. Interaction of phospholipids with proteins, peptides and amino acids. Advances 1987–1989. *Int. J. Biochem.* 23:131–145.

Cserhåti, T., and M. Szögyi. 1992. Interaction of phospholipids with proteins and peptides. New advances 1990. *Int. J. Biochem.* 24:525–538.

Cserhåti, T., and M. Szögyi. 1993. Interaction of phospholipids with proteins and peptides. New advances 3. *Int. J. Biochem.* 25:123–146.

Davis, J. H., D. M. Clare, R. S. Hodges, and M. Bloom. 1983. Interaction of a synthetic amphiphilic polypeptide and lipids in a bilayer structure. *Biochemistry.* 22:5298–5305.

Epand, R. M., and R. F. Epand. 1992. Lipid-peptide interactions. *In* The Structure and Function of Biological Membranes. P. Yeagle, editor. CRC Press, Boca Raton, Florida. 573–601.

Gennis, R. B. 1989. Biomembranes: Molecular Structure and Function, Springer-Verlag, New York.

Huschilt, J. C., R. S. Hodges, and J. H. Davis. 1985. Phase equilibria in an amphiphilic peptide-phospholipid model membrane by deuterium nuclear magnetic resonance difference spectroscopy. *Biochemistry.* 24: 1377–1386.

Huschilt, J. C., B. M. Millman, and J. H. Davis. 1989. Orientation of α-helical peptides in a lipid bilayer. *Biochim. Biophys. Acta.* 979: 139–141.

Lewis, B. A., and D. M. Engelman. 1983. Bacteriorhodopsin remains dispersed in fluid phospholipid bilayers over a wide range of bilayer thicknesses. *J. Mol. Biol.* 166:203–210.

Lewis, R. N. A. H., and R. N. McElhaney. 1993. Calorimetric and spectroscopic studies of the polymorphic phase behavior of a homologous series of *n*-saturated 1,2-diacyl phosphatidylethanolamines. *Biophys. J.* 64:1081–1096.

Mantsch, H. H., C. Madec, R. N. A. H. Lewis, and R. N. McElhaney. 1985. Thermotropic phase behavior of model membranes composed of phosphatidylcholines containing isobranched fatty acids. 2. Infrared and 31P-NMR spectroscopic studies. *Biochemistry.* 24: 2440–2446.

Mantsch, H. H., and R. N. McElhaney. 1991. Phospholipid phase transitions in model and biological membranes as studied by infrared spectroscopy. *Chem. Phys. Lipids.* 57:213–226.

McElhaney, R. N. 1982. The use of differential scanning calorimetry and differential thermal analysis in studies of model and biological membranes. *Chem. Phys. Lipids.* 30:229–257.

McElhaney, R. N. 1986. Differential scanning calorimetric studies of lipid-protein interactions in model membrane systems. *Biochim. Biophys. Acta.* 864:361–421.

Mendelsohn, R., and H. H. Mantsch. 1986. Fourier transform infrared studies of lipid-protein interactions. *In* Progress in Lipid Protein Interaction, Vol. 2. A. Watts and J. J. H. M. Depont, editors. Elsevier, Amsterdam. 103–146.

Morrow, M. R., J. C. Huschilt, and J. H. Davis. 1985. Simultaneous modeling of phase and calorimetric behavior in an amphiphilic peptide/phospholipid model membrane. *Biochemistry.* 24:5396–5406.

Mouritsen, O. G., and M. Bloom. 1984. Mattress model of lipid-protein interaction in membranes. *Biophys. J.* 46:141–153.

Nagle, J. F. 1976. Theory of lipid monolayer and bilayer phase transitions: effect of headgroup interactions. *J. Membr. Biol.* 27:233–250.

Owicki, J. C., and H. M. McConnell. 1979. Theory of protein-lipid and protein-protein interactions in bilayer membranes. *Proc. Natl. Acad. Sci. USA.* 76:4750–4754.

Pauls, K. P., A. L. MacKay, O. Söderman, M. Bloom, A. K. Taneja, and R. S. Hodges. 1985. Dynamic properties of the backbone of an integral membrane polypeptide measured by ^{2}H-NMR. *Eur. Biophys. J.* 12:1–11.

Peschke, J., J. Riegler, and H. Möhwald. 1987. Quantitative analysis of membrane distortion induced by mismatch of protein and lipid hydrophobic thickness. *Eur. Biophys. J.* 14:385–391.

Riegler, J., and H. Möhwald. 1986. Elastic interactions of photosynthetic reaction center proteins affecting phase transitions and protein distributions. *Biophys. J.* 49:1111–1118.

Roux, M. R., J. M. Neumann, R. S. Hodges, P. F. Devaux, and M. Bloom 1989. Conformational changes of phospholipid headgroups induced by a cationic integral membrane peptide as seen by deuterium magnetic resonance. *Biochemistry.* 28:2313–2321.

Selinsky, B. S. 1992. Protein-lipid interactions and membrane function. *In* The Structure and Function of Biological Membranes. P. Yeagle, editor. CRC Press, Boca Raton, Florida. 603–651.

Sperotto, M. M., and O. G. Mouritsen. 1988. Dependence of lipid membrane phase transition temperature on the mismatch of protein and lipid hydrophobic thickness. *Eur. Biophys. J.* 16:1–10.

Sperotto, M. M., and O. G. Mouritsen. 1991. Monte Carlo simulation studies of lipid order parameter profiles near integral membrane proteins. *Biophys. J.* 59:261–270.

Watts, A., and J. J. H. H. M. DePont, editors. 1985. Progress in Lipid Protein Interactions, Vol. 1. Elsevier, Amsterdam.

Watts, A., and J. J. H. H. M. DePont, editors. 1986. Progress in Lipid Protein Interactions, Vol. 2. Elsevier, Amsterdam.

Yeagle, P. 1992. The Structure of Biological Membranes, CRC Press, Boca Raton, Florida.

Zhang, Y-P., R. N. A. H. Lewis, R. S. Hodges, and R. N. McElhaney. 1992a. FTIR spectroscopic studies of the conformation and amide hydrogen exchange of a peptide model of the hydrophobic transmembrane α-helices of membrane proteins. *Biochemistry.* 31:11572–11578.

Zhang, Y-P., R. N. A. H. Lewis, R. S. Hodges, and R. N. McElhaney. 1992b. Interaction of a peptide model of a hydrophobic transmembrane α-helical segment of a membrane protein with phosphatidylcholine bilayers: differential scanning calorimetric and FTIR spectroscopic studies. *Biochemistry.* 31:11579–11588.